Exp.-Nr. A2-12/05
Eingang: 25.08.05
an PAC:

Mainz Microtron MAMI

Collaboration A2: "Real Photons"
Spokesperson: A. Thomas

Proposal for an Experiment

Measurement of polarization observables in coherent π^0 photoproduction off deuterium

Collaborators :

CrystalBall@MAMI collaboration

I. Strakovsky, The George Washington University

A. Kudryavtsev, V. Tarasov and V. Baru, ITEP (Moscow)

A. Fix, Johannes Gutenberg-Universität Mainz (Germany)

Spokespersons for the Experiment :

Y. Y. Ilieva, The George Washington University
W. J. Briscoe, The George Washington University
B. Krusche, University of Basel

Abstract of Physics :

We propose to measure unpolarized differential cross section $\frac{d\sigma}{d\Omega}$ and single-polarization observables Σ, T_{20}, iT_{11}, T_{21}, T_{22} of the reaction $\gamma d \to \pi^0 d$ at backward pion CM angles and photon energies between 0.5 and 1.4 GeV. The photon energy range between 0.6 and 0.8 GeV is of special interest since at these energies the coherent process shows strong sensitivity to intermediate η-rescattering mechanism through the excitation of $S_{11}(1535)$. Also, for $\cos(\theta^{\pi}_{CM}) < -0.25$, the invariant cross sections show a general scaling with s^{13} (as predicted by dimensional counting rules) at non-perturbative kinematics. High statistics measurement of unpolarized differential cross section and polarization observables of the reaction $\gamma d \to \pi^0 d$ will allow for better understanding of the above two phenomena.

Abstract of Equipment :

Tagged unpolarized photon beam on an unpolarized LD_2 target, as well as on polarized deuterium target with polarization axis oriented longitudinally, transversely and at an angle of 54.7° with respect to the photon beam. The alignment of the longitudinally-polarized-target polarization axis with respect to the beam axis must be better than 1°. We will use the combination of the Crystall Ball detector and the TAPS spectrometer.

MAMI–Specifications :

beam energy	1500 MeV
beam current	$<$ 100nA
time structure	cw
polarization	unpolarized/linearly polarized photons

Experiment–Specifications :

experimental hall/beam	A2
detector	Crystal Ball, TAPS, MWPC, PID
target material	LD_2, polarized deuterium

Beam Time Request :

set–up without beam	200 hours
set–up/tests with beam	200 hours (parallel with proposal A2/ ???)
data taking	2275 hours (1075 parallel with proposal A2/ ???)

1 Introduction

The deuteron is the simplest bound two-nucleon system in nature. Thus, it is of fundamental importance for understanding the properties of light nuclei and reactions involving light nuclei. The deuteron has been vigourosly studied in the past decades, and a lot of progress has been made on the theoretical side for providing highly reliable deuteron wave functions.
Studying the reaction $\gamma d \to \pi^0 d$ at present time seems to be particularly fruitful since it coincides with intensive research of the elementary amplitude $\gamma N \to \pi^0 N$ via single and double polarization experiments at JLab and MAMI, aiming to determine the helicity amplitudes with very high precision up to around 2 GeV. Thus, the knowledge of the deuteron wave functions and the elementary photoproduction process gives better perspective for the study of $\gamma d \to \pi^0 d$ and interpretation of experimental data.
The main problem for understanding the underlying reaction dynamics is to define the effective degrees of freedom relevant at specific kinematics. At lower energies, close to threshold and in the first resonance region, the coherent process is well described in terms of meson-nucleon degrees of freedom. At medium energies, and moderate momentum transfer to the deuteron (above 1 GeV^2) current meson-nucleon models fail to reproduce the unpolarized differential cross sections. This momentum-transfer range is problematic since the impulse approximation (IA) alone is not sufficient to describe the reaction dynamics and other mechanisms need to be included in the theory. The possibility for substantial contributions from a two-step process - mainly meson rescattering in the intermediate state from the second nucleon, is a complication with respect to the description of the photoproduction on a single nucleon. Also, there are basically no measurements of polarization observable of $\gamma d \to \pi^0 d$ to constrain the models. On the other hand, at high s and large t the probe should become sensitive to the quark-gluon structure of the nucleons in the deuteron. The transition between meson-nucleon and quark-gluon degrees of freedom has been long standing problem in the medium energy physics, which is still unresolved. QCD has been very successful at high energies, where perturbative treatment can be applied. At moderate momentum transfer, however, non-perturbative effects are important.
The key importance of the coherent pion photoproduction on the deuteron for understanding similar processes on the three- and four- nucleon systems, combined with the unique opportunity provided by the current high-precision studies of the elementary process at few research labs, and the theoretical advance in understanding the deuteron wave function, make a detailed study of the reaction $\gamma d \to \pi^0 d$ at medium energies very appealing.

2 Scientific motivation

2.1 Reaction dynamics close to the η-photoproduction threshold on a single nucleon

The reaction $\gamma d \to \pi^0 d$ is characterized by high momentum transfer at pion backward CM angles which makes it very suitable for studying the role of meson-rescattering mechanisms in the cross section. At high t, meson-rescattering is expected to have a dominant contribution to the total amplitude since it allows for the momentum transfer to be shared among the two nucleons, and this is energetically more efficient than for a single nucleon to absorb all of the transferred momentum.
Recent CLAS measurement of the reaction $\gamma d \to \pi^0 d$ [1], as well as previous data [2], clearly

show a disagreement with the impulse approximation [3] at pion backward CM angles. A typical rescattering process, considered to be important at high t, is a pion rescattering in the intermediate state [3], [4]. However, this has proved to be insufficient for describing the experimental cross sections. Especially, in the vicinity of $E_\gamma = 0.7$ GeV where both [1] and [2] show well pronounced enhancement for $\cos(\theta^\pi_{CM}) < -0.65$ which gets broader when increasing the pion CM angle (see Fig. 1). Thus, one must account for another mechanism which has a

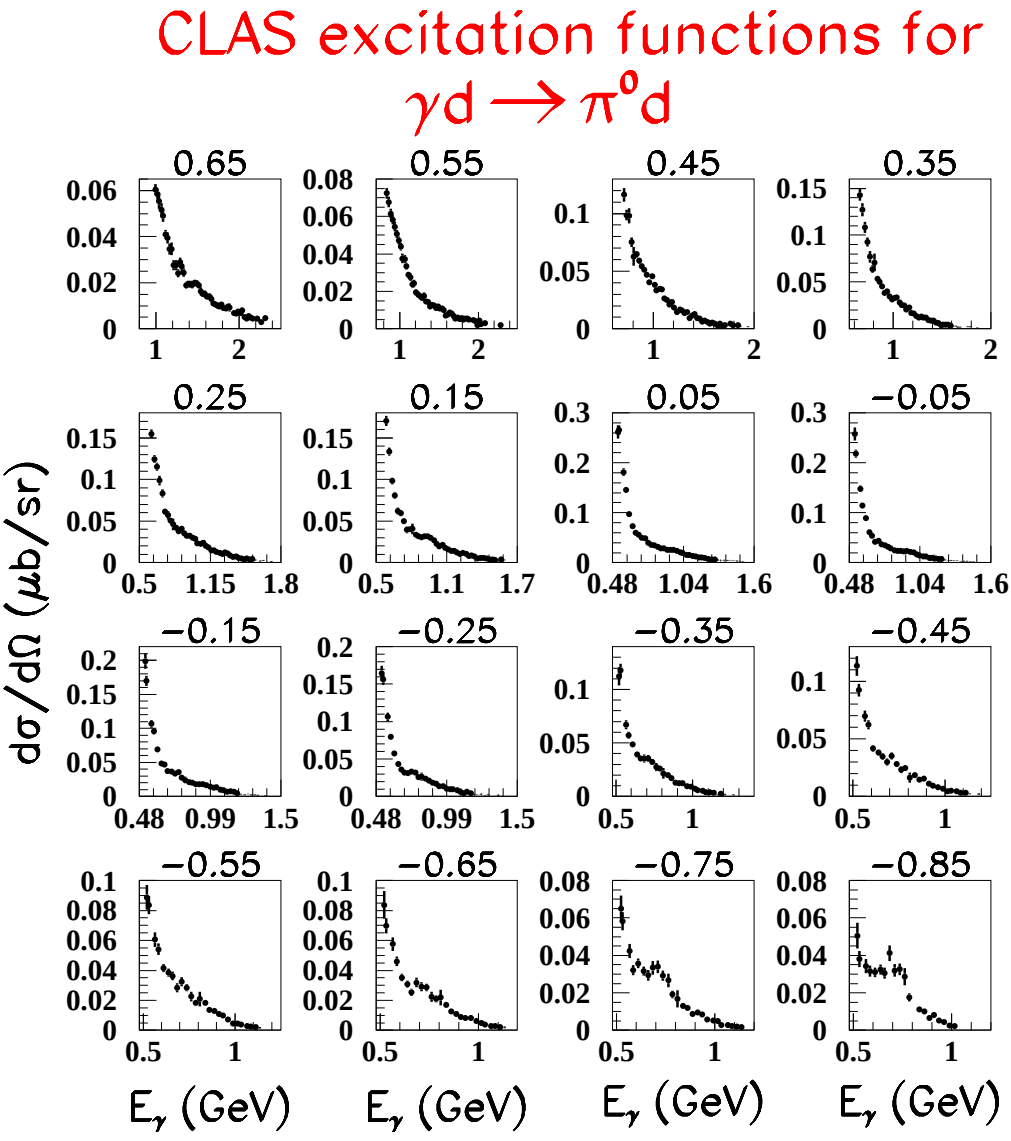

Figure 1: CLAS excitation functions [1] for $\gamma d \to \pi^0 d$ for various $\cos(\theta^\pi_{CM})$ values (shown on top of the plots). In general, the excitation functions are featureless, except for $\cos(\theta^\pi_{CM}) < -0.65$, where a well pronounced structure can be seen near $E_\gamma = 0.7$ GeV.

relatively large contribution in this kinematical range.
Since 0.7 GeV is the threshold for η photoproduction on a single nucleon, it is natural to assume that the observed structure in the excitation function is due to the opening of the ηN threshold and, therefore, to a contribution from intermediate η-rescattering.
Close to threshold, the ηN interaction is governed by the s-wave resonance $N^*(1535)$. This makes the s-wave part of the ηN interaction considerably large and leads to large cross section close to the ηN threshold. Since the coupling $S_{11}(1535) \to \eta N$ is larger than $S_{11}(1535) \to \pi N$, the main contribution to the structure observed in the $\gamma d \to \pi^0 d$ data should come from intermediate η-rescattering, rather than from π-rescattering [5].
A dominating s-wave contribution to the reaction amplitude should lead to more isotropic differential cross sections. This is actually shown by the differential cross sections [1] at backward pion angles for the photon energies where the structure is observed (see Fig. 2).
A phenomenological model for $\gamma d \to \pi^0 d$ [5] shows that the amplitude corresponding to the Feynman diagram in Fig. 3 can produce visible enhancement of the excitation function near the η threshold at large pion CM angles. The enhancement is mainly due to the $S_{11}(1535)$ contributions in the elementary amplitudes of the double-scattering diagram. Current fits to the CLAS data, based on the model [5] (see Fig. 4), show that the excitation functions at backward pion angles are very well described by an exponential background and the rescattering process shown in Fig. 3. A good χ^2/ndf, however, is achieved only when account is taken of interference between the two processes.
Second-order ηN interaction, represented by the Feynman diagram shown in Fig. 5, might also contribute to the excess of differential cross section close to the η threshold [6]. This has been shown to be important for threshold coherent and incoherent η photoproduction off the deuteron in a recent study of the ηNN contribution to these processes [7]. Fig. 6 shows qualitative predictions from the model of [6] for the unpolarized cross sections. One can see that the structure is not reproduced at 90°, as shown by the data and the other model [5]. It is an interesting observation, that the IA alone can produce a structure at 0.7 GeV. The contribution from 2- and 3- step processes involving η-rescattering change the shape of the excitation function, enhancing the signal. The study of the amplitudes of the rescattering processes shown in Figures 3 and 5 is also important with respect to searches for η-mesic nuclei, since these are the main mechanisms through which a formation of a bound η-nucleus state can proceed [8].
In order to study the amplitudes of the above rescattering mechanisms, and especially to evaluate their relative contributions, one needs to collect data with higher statistical accuracy than the data of [1] (less than 5% in the energy range of the structure). Polarization observables are more sensitive to the reaction dynamics, and especially to interference between different amplitudes, and will give a better quantitative description of the rescattering subprocesses.

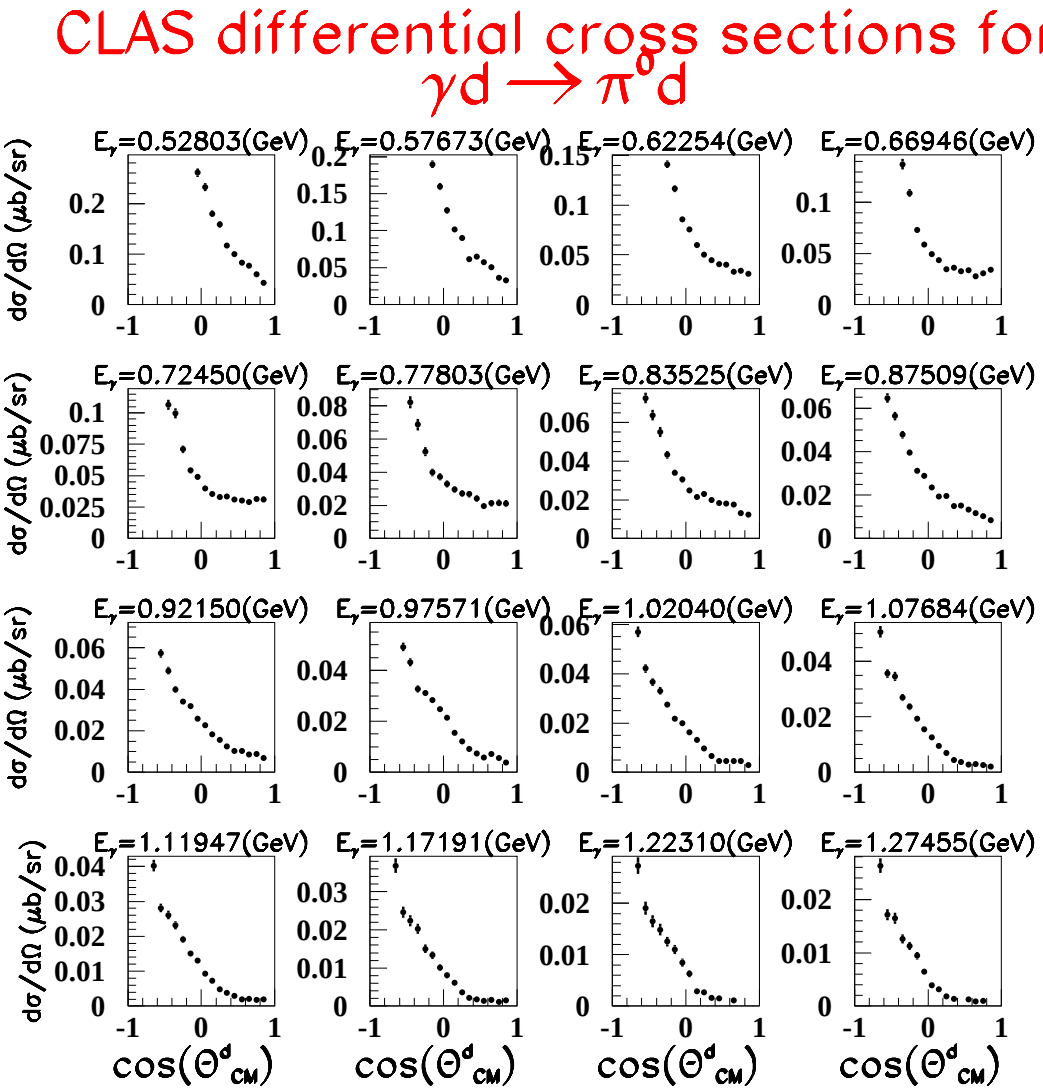

Figure 2: CLAS differential cross sections for $\gamma d \to \pi^0 d$ for various photon energy values (shown on top of the plots). One can see the effect of the opening of the ηN threshold in the flattening of the cross sections at E_γ between 0.6 and 0.8 GeV and $\cos(\theta^\pi_{CM}) < -0.6$. A similar effect is observed at $E_\gamma > 0.9$ GeV, but there is different physics behind it.

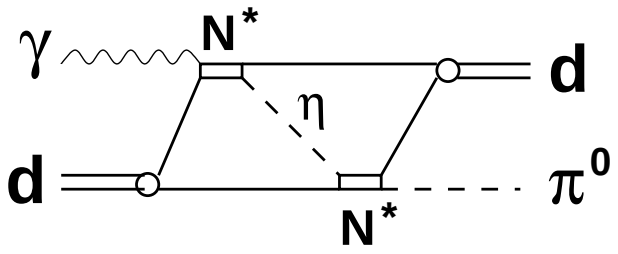

Figure 3: Double-scattering diagram with intermediate η production leading to an enhancement of the excitation function of $\gamma d \to \pi^0 d$ at large pion CM angles near photon energy of 0.7 GeV.

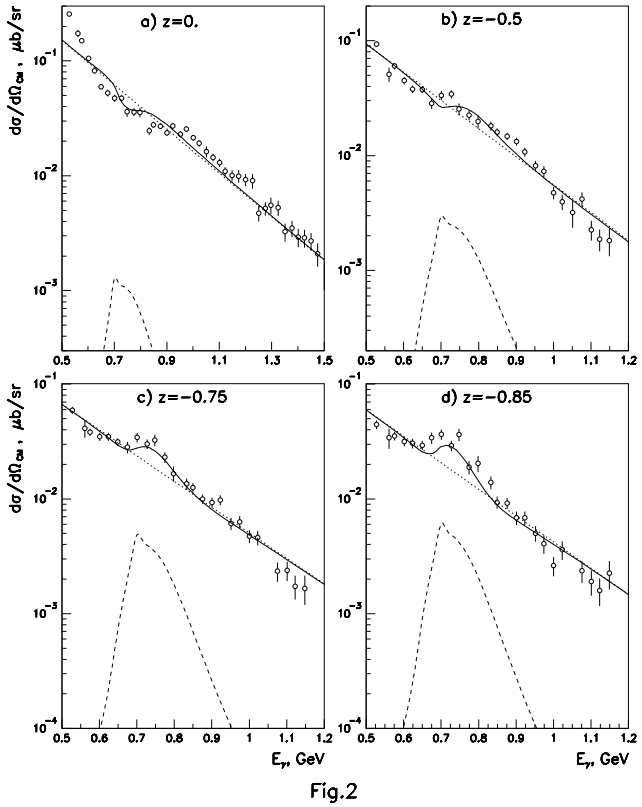

Figure 4: Fits to the data [1], based on the model [5]. Interference term between the η-rescattering mechansim and the background is taken into account. z denotes $\cos(\theta^{\pi}_{CM})$. The data are binned in 25.5-MeV wide photon-energy bins.

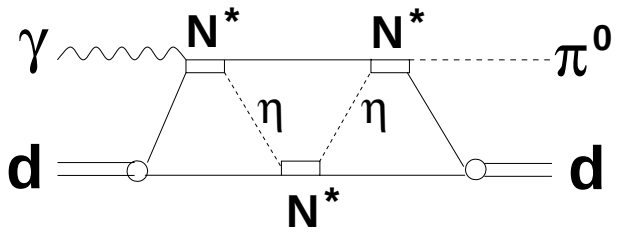

Figure 5: Higher-order rescattering diagram which might contribute to the enhancement near photon energy of 0.7 GeV.

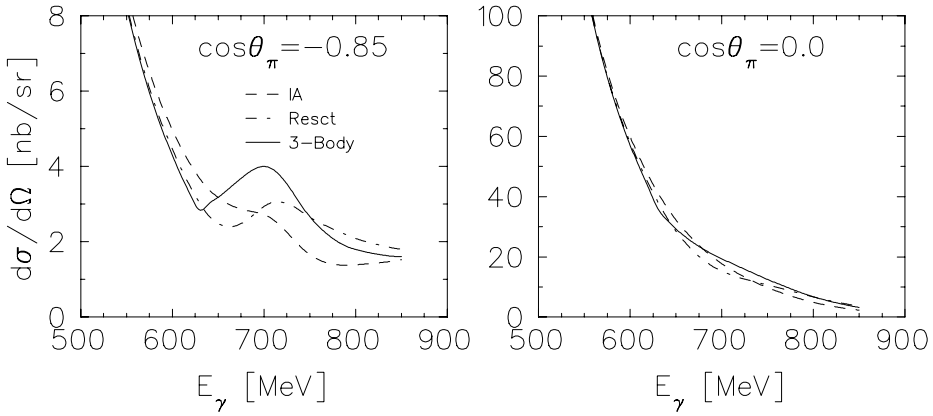

Figure 6: Predictions from the model [6] for the unpolarized cross sections of $\gamma d \to \pi^0 d$ for $\cos(\theta^{\pi}_{CM})$=-0.85 and 0.

2.2 Study of the scaling properties of the invariant cross sections between 0.5 and 1.6 GeV at backward pion CM angles

Understanding the reaction dynamics of exclusive processes at moderate and high momentum transfer has been a long-standing problem in the medium-energy physics. Traditional meson-nucleon models are quite successful up to a momentum transfer of around 1 $(\mathrm{GeV}/c)^2$, but fail to predict the data at higher t. Currently, non-perturbative QCD approaches are not in a state to be applied to medium-energy nuclear reactions. Therefore, in the recent years the question about applying pQCD to exclusive processes at moderate t has been widely discussed. It was shown by Brodsky *et al.* [9] that the reaction $\gamma d \to \pi^0 d$ is a good choice of an exclusive process for testing the scaling prediction of the Constituent Counting Rule (CCR) and the applicability of the Reduced Nuclear Amplitude (RNA) approach.
The CCR states that in the asymptotic limit of $t \to \infty$ the invariant cross section for an exclusive process of the type $A + B \to C + D$ scales as:

$$\frac{d\sigma}{dt} \sim \frac{1}{s^{n-2}} f(\theta_{CM}),$$

where t and s are the square of the four-momentum transfer, and the total CM energy, respectively, and n is the total number of the initial and final elementary fields. In the case of coherent pion photoproduction on deuterium $n - 2 = 13$.
According to the RNA formalism, the invariant amplitude $\mathcal{M}_{\gamma d \to \pi^0 d}$ can be factorized as [9]:

$$\mathcal{M}_{\gamma d \to \pi^0 d}(u,t) = C' f_d(t) \mathcal{M}_{\gamma N \to \pi^0 N}(u/4, t/4) F_{N_2}(t/4), \tag{1}$$

where C' is a constant, $f_d(t)$ is the reduced deuteron form factor, $F_{N_2}(t/4)$ is the nucleon form factor at half the momentum transfer, and $\mathcal{M}_{\gamma N \to \pi^0 N}(u/4, t/4)$ is the amplitude of the elementary pion photoproduction on a single nucleon. The latter two are taken at half the momentum transfer, since for vanishing nuclear binding energy the deuteron can be regarded as two nucleons sharing, to first approximation, the momentum transfer equally. The RNA formalism provides an extension of pQCD predictions to exclusive processes involving nuclei, since soft effects related to the nuclear and nucleon structures are accounted for by factoring out the corresponding electromagnetic form factors.
The CLAS data show that the invariant amplitude for $\gamma d \to \pi^0 d$ does not factorize up to a beam energy of 0.9 GeV. Above 0.9 GeV, the RNA factorization seems to work well for $\cos(\theta^{\pi}_{CM}) \leq$ -0.65. This kinematic range corresponds to the highest momentum transfers we have access to with the CLAS data set. This feature means that the relative contribution of two-step processes, such as intermediate meson rescattering, to the reaction cross section becomes small at high t when the beam energies are above 0.9 GeV. It will be interesting to have data at higher beam energies which would extend the momentum transfer range, in order to observe if the consistency between the data and the RNA prediction is a stable trend.
Linear fits to the logarithmic dependence of the invariant cross sections on s of the CLAS data show a general scaling, with the power of s of 13, as predicted by CCR, for $\cos(\theta^{\pi}_{CM}) > -0.25$ (see Figs. 7 and 8). The scaled invariant cross sections show local variations around a constant value, when increasing s. The consistency between the experimental data and the quark counting rule predictions is confirmed by a measurement of the same reaction in Hall-C at JLab [10] at $\theta^{\pi}_{CM} = 136^{\circ}$ and E_{γ} up to 2.5 GeV.
Now, the applicability of pQCD to medium-energy exclusive processes is currently highly controversial. On the other hand many hadronic and electromagnetic processes (πp elastic scattering,

πd elastic scattering, real Compton scattering off the proton, pion photoproduction off the nucleon, *etc.*) exhibit variating scaling with the predicted by the CCR power of s already at moderate momentum transfer. This behaviour is an interesting phenomenon itself, since it surprisingly happens in the non-perturbative domain and is consistently shown by many nuclear reactions. It seems that there is a more fundamental physics behind.

There are several assumptions about the nature of the reaction mechanisms leading to different power fall off behaviour of the invariant cross section. These may be contributions from spin-flip amplitudes, or interferences between soft and hard amplitudes.

It is worth mentioning that the meson-nucleon models for the reaction $\gamma d \to \pi^0 d$, [3] and [4], do not reproduce the energy dependence of the invariant cross section above photon energy of ~ 0.7 GeV, and thus, cannot explain the observed scaling.

We think that the proper way to understand the nature of the scaling observed in medium-energy exclusive processes is to understand the underlying reaction dynamics, *i.e.* to evaluate helicity amplitudes through polarization measurements, and study their interference' energy dependence.

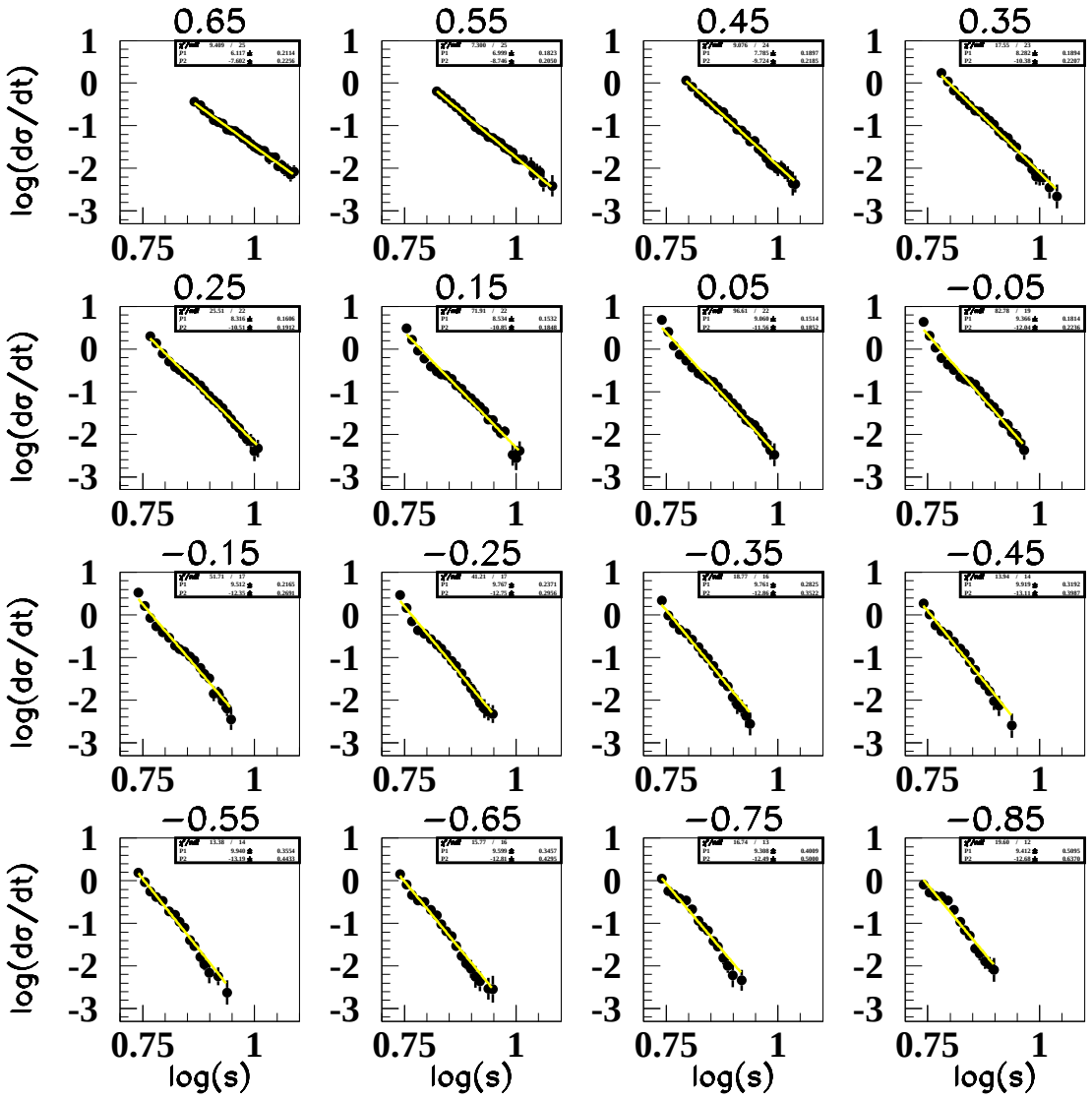

Figure 7: Fits to the CLAS invariant cross sections, as a function of s, for different $\cos(\theta^{\pi}_{CM})$ (shown on top of the plots). One can see that $\log(\frac{d\sigma}{dt})$ is almost linear with $\log(s)$ for fixed CM angle. The slope of the line decreases as the pion CM angle increases and reaches the value of 13 at $\cos(\theta^{\pi}_{CM}) = -0.25$.

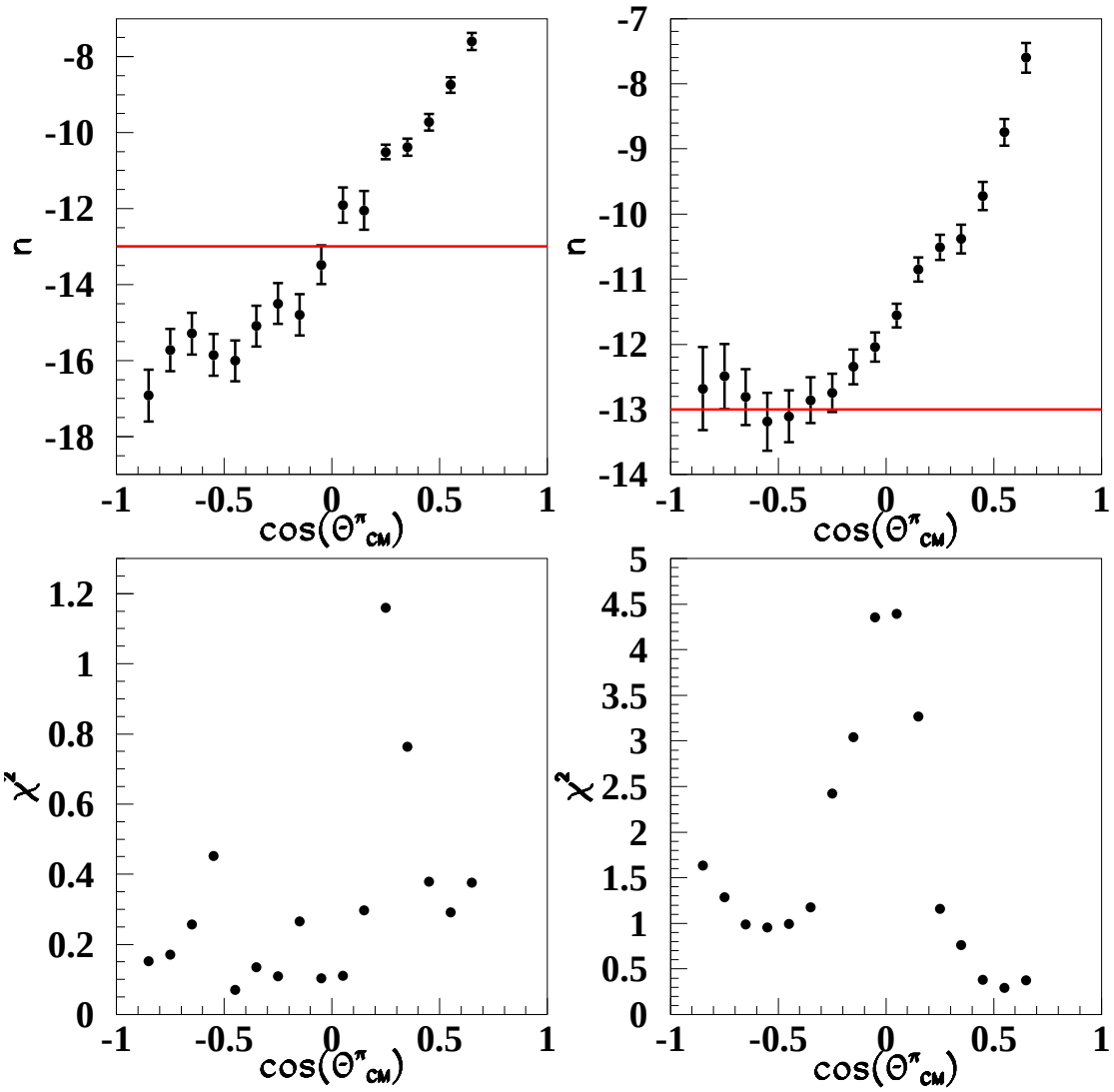

Figure 8: The parameter n, extracted from the fits shown in the previous figure, for $\frac{d\sigma}{dt} = a \times s^n$. Left top: the parameter n when only data at $t > 1$ (GeV/c)^2 are fitted; bottom left: χ^2/ndf for these fits. Top right: parameter n when the complete data set is fitted; bottom right: χ^2/ndf for these fits. These plots contain a quantitative estimate of the variation of the scaling shown by the CLAS data.

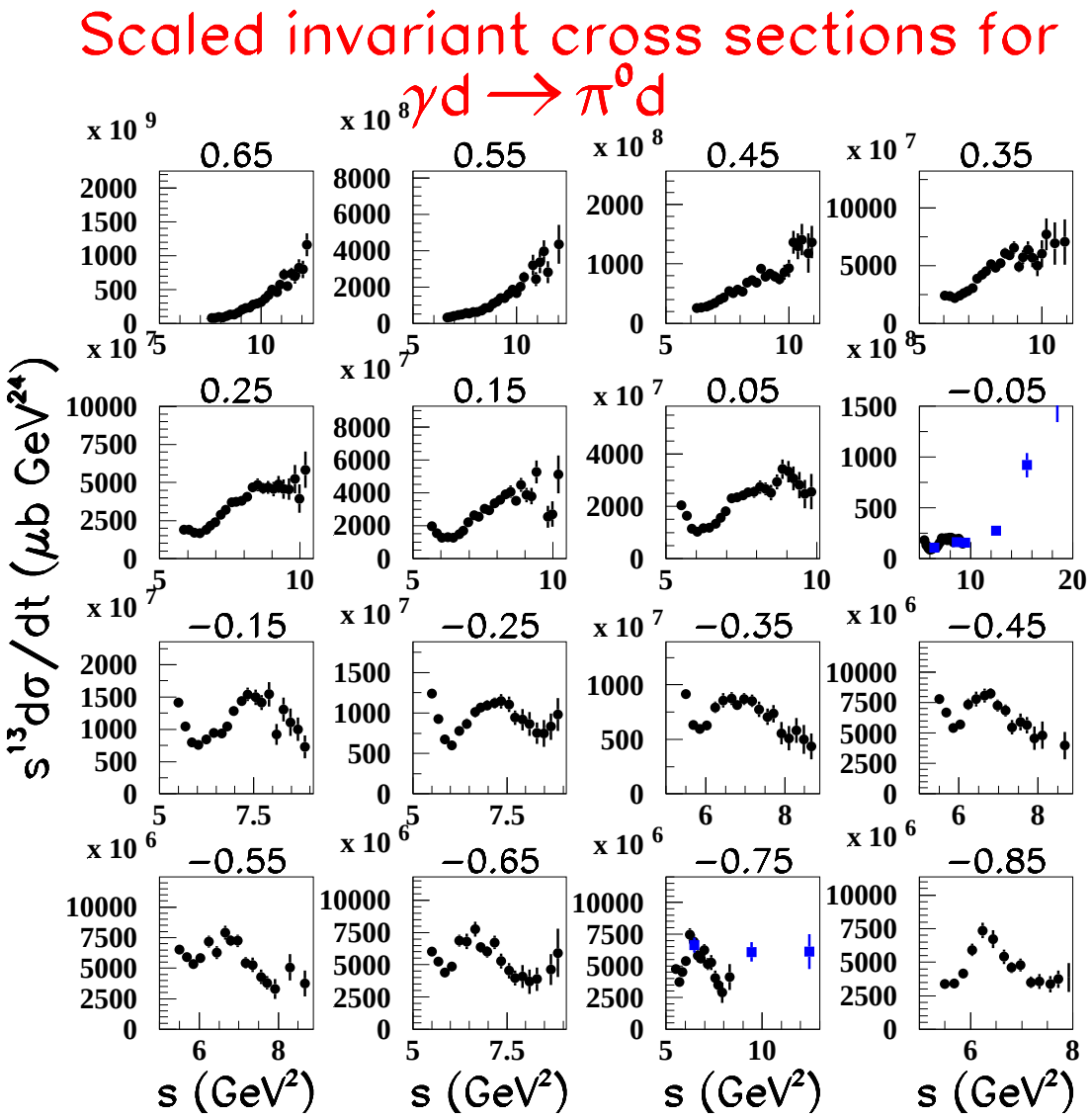

Figure 9: Scaled invariant cross sections for $\gamma d \to \pi^0 d$ as a function of s. The blue squares are from [10]. The data show the variation scaling at $\cos(\theta^{\pi}_{CM}) < -0.25$ over the energy range covered by the CLAS experiment.

The reaction $\gamma d \to \pi^0 d$ has 9 independent helicity amplitudes, which require 17 independent measurements in order to reconstruct them. So far, there is no comprehensive polarization measurement of this process at photon energies above 0.5 GeV, covering large CM angular range.
An analysis of this process at $\theta^{\pi}_{CM} = 180°$, in terms of helicity apmplitudes, is much less complicated since many of them cancel out. In this sense, the fact that the combined detector

system Crystal Ball-TAPS has an angular coverage in terms of polar LS angle already at 3° is a great opportunity.
We will use the unique capabilities of the detector system: Cristall Ball-TAPS, to measure the reaction $\gamma d \to \pi^0 d$ at photon energies between 0.5 and 1.6 GeV and pion backward CM angles.

3 Polarization observables

As mentioned before, the reaction $\gamma d \to \pi^0 d$ has 9 independent helicity amplitudes $A_{\lambda_i \lambda_f}$ corresponding to initial photon helicity λ_γ=1 and initial and final deuteron helicities λ_i and λ_f, respectively. The differential cross section in CM can be expressed in terms of $A_{\lambda_i \lambda_f}$ as following

$$\frac{d\sigma}{d\Omega} = \frac{1}{64\pi^2 s}\frac{|\vec{q}|}{|\vec{k}|}\frac{1}{6}2\sum_{\lambda_i,\lambda_f}|A_{\lambda_i\lambda_f}|^2 \tag{2}$$

The initial state polarization observables Σ (photon asymmetry), iT_{11} (vector analyzing power of the deuteron), and T_{20}, T_{21} and T_{22} (tensor analysing powers of the deuteron) are given in terms of the helicity amplitudes [4] by

$$\Sigma = \frac{4}{Tr}Re[A^*_{11}A_{-1-1} - A^*_{10}A_{-10} + A^*_{1-1}A_{-11} - A^*_{01}A_{0-1} + |A_{00}/2], \tag{3}$$

$$iT_{11} = \frac{\sqrt{6}}{Tr}Im[A^*_{0-1}A_{1-1} + A^*_{00}A_{10} + A^*_{01}A_{11} - A^*_{01}A_{-11} - A^*_{00}A_{-10} - A^*_{0-1}A_{-1-1}], \tag{4}$$

$$\begin{aligned} T_{20} = \frac{\sqrt{2}}{Tr}[&|A_{1-1}|^2 + |A_{10}|^2 + |A_{11}|^2 + |A_{-11}|^2 + |A_{-10}|^2 + |A_{-1-1}|^2 \\ &-2(|A_{-1-1}|^2 + |A_{00}|^2 + |A_{01}|^2)], \end{aligned} \tag{5}$$

$$T_{21} = -\frac{\sqrt{6}}{Tr}Re[A^*_{0-1}A_{1-1} + A^*_{00}A_{10} + A^*_{01}A_{11} - A^*_{01}A_{-11} - A^*_{00}A_{-10} - A^*_{0-1}A_{-1-1}], \tag{6}$$

$$T_{22} = \frac{2\sqrt{3}}{Tr}Re[A^*_{-1-1}A_{1-1} + A^*_{-10}A_{10} + A^*_{-11}A_{11}], \tag{7}$$

where $Tr = 2\sum_{\lambda_i,\lambda_f}|A_{\lambda_i\lambda_f}|^2$.
In case of an experiment with a polarized target and unpolarized beam, the differential cross section $\sigma(\theta)$ can be expressed in terms of the unpolarized cross section $\sigma_0(\theta)$ and the target analyzing powers [11]

$$\begin{aligned} \sigma(\theta) = \sigma_0[1 + &iT_{11}(\theta)\sqrt{3}p_z \sin\beta\cos\varphi + \frac{1}{2\sqrt{2}}T20(\theta)p_{zz}(3\cos^2\beta - 1) \\ &+\sqrt{3}T_{21}(\theta)p_{zz}\sin\beta\cos\beta\sin\varphi \\ &-\frac{\sqrt{3}}{2}T_{22}(\theta)p_{zz}\sin^2\beta\cos 2\varphi], \end{aligned} \tag{8}$$

where p_z and p_{zz} are the target vector and tensor polarization along the quantization axis $O\hat{Z}$, and β and φ are the Euler angles of the quantization axis (the target magnetic field axis). The 4 analyzing powers are real, due to parity conservation. For the same reason T_{10} =0.

The coordinate frame of the scattering, in accordance with the Madison convention, is shown in Fig. 10. The z axis is along the incident photon momentum $\vec{P}_\gamma$, the y axis is along $\vec{P}_\gamma \times \vec{P}_d$, and the x axis is then along $\hat{y} \times \hat{z}$. β is the angle between the quantization axis and the z axis; φ is the angle between the y axis and the quantization axis projection in the xy plane. In a coordinate system where the y axis is along that projection, the angle φ is the azymuthal angle of the scattered deuteron.

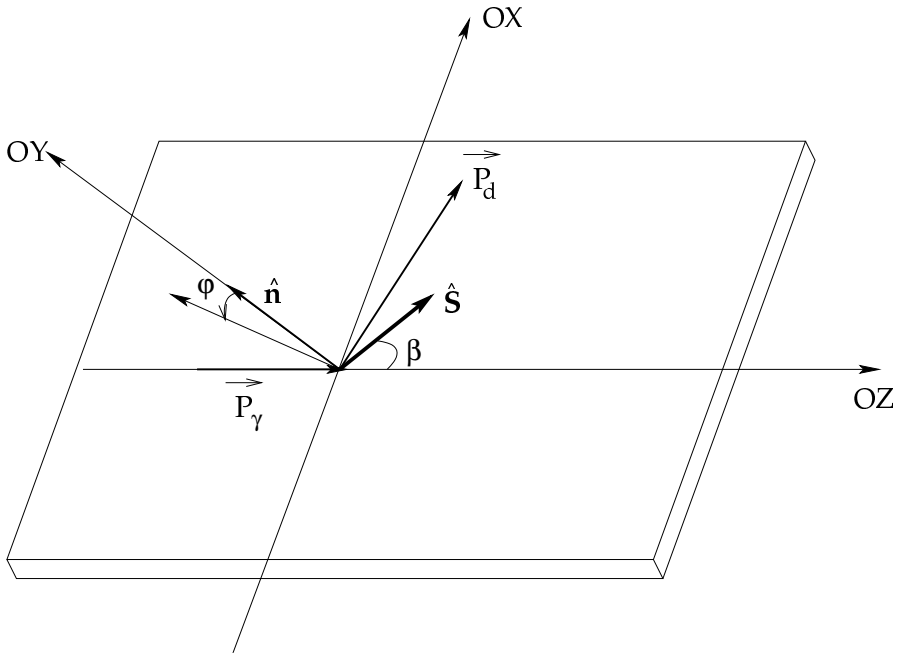

Figure 10: Coordinate system xyz in which the polarization state of the polarized deuteron target is described; the incident photon momentum $\vec{P}_\gamma$ is along $+z$; the normal $\hat{\mathbf{n}} = \vec{P}_\gamma \times \vec{P}_d$ is along $+y$. The spin alignment axis $\hat{\mathbf{s}}$ makes angle β with the OZ axis; its projection in the xy plane makes angle φ with the OY axis.

Being a massive particle with spin 1, the deuteron has three magnetic substates m=±1,0. Denoting the population of these substates by n^+, n^-, and n^0, the vector and tensor polarizations of the target can be expressed as

$$p_z = \frac{n^+ - n^-}{n^+ + n^- + n^0}$$

$$p_{zz} = \frac{n^+ - n^- - 2n^0}{n^+ + n^- + n^0} = \frac{1 - 3n^0}{n^+ + n^- + n^0},$$

where the normalization $n^+ + n^- + n^0 = 1$ is used. Provided the populations of the three magnetic substates can be described by a Boltzmann distribution, and one can neglect the effects of the deuteron quadrupole moment, the tenzor polarization can be derived from the vector polarization from the following relation

$$p_{zz} = 2 - \sqrt{4 - 3p_z^2} \tag{9}$$

In case when the target is unpolarized and the photon beam is linearly polarized with polarization axis in the xy plane

$$\sigma(\theta) = \sigma_0(\theta)[1 + P_{lin}\Sigma(\theta)cos2\varphi], \tag{10}$$

where P_{lin} is the polarization of the beam.

In order to determine experimentally the helicity amplitudes (up to an overall phase) of the reaction $\gamma d \to \pi^0 d$, one needs to do 17 independent measurements. Double polarization observables, such as polarization correlation parameters (polarized beam and target) or polarization-transfer parameters (polarized beam, or target, and polarization of one of the final-state particles), must be measured in addition to the above single polarization observables. Large kinematical coverage is a must as well. This is an enormous task and it becomes only possible due to the development of high intensity beams, solid-state polarized deuterium targets, and 4π detectors.
So far, there is no comprehensive polarization measurement of the reaction $\gamma d \to \pi^0 d$ at photon energies above 0.5 GeV covering large CM angular range and this is largely an unexplored domain. There are several published data on the beam analyzing power Σ at few backward pion CM angles which are shown in Fig. 11 (the figure is taken from [12]). The data are compared with the model prediction of [4] and the figure shows the sensitivity of the observable to changes in the deuteron wave function.
Theoretical predictions within the model of [4] for the energy dependence of Σ at pion CM angle of 90°, 130°, and 135° are shown in Fig. 12. Based on the studies of [4], one concludes that the polarization observable Σ is very sensitive to small components of the deuteron wave function and, to a lesser extent, to the elementary photoproduction amplitude, especially in the region 0.6–0.8 GeV. However, this is the energy range where the η-structure is observed in the CLAS unpolarized cross sections and in backward πd elastic scattering. Thus, there is another interpretation of the observed structures. An interesting feature of the existing data is a minimum and a change of slope of Σ in that region. It is necessary to measure this observable at other angles and higher energies, above the region of the η-structure. Fig. 13 shows predictions for Σ and the target analyzing powers iT_{11}, T_{20}, and T_{21} for E_γ=0.6 GeV from the model [4]. One can see that T_{20} is the most sensitive variable to changes in the model, especially at pion CM angles above 150°. These angles are beyond the capabilities of CLAS. Thus, the combination of the CB-TAPS is extremely favorable for studying this interesting angular range. The vector analyzing power iT_{11} shows the least sensitivity to changes in the model, whereas T_{20}, and T_{22} are more sensitive at slightly lower angles. One needs to mention that due to parity conservation, Σ, iT_{11}, and T_{21} vanish at forward and backward angles. There are no measurements of the target analyzing powers for $\gamma d \to \pi^0 d$ above 0.5 GeV.

4 Experimental Setup

4.1 Detector

We will make use of the combined detector Crystal Ball-TAPS, which has a close to 4π angular acceptance and allows particle detection at as low as 3° in LS. The photons from the pion decay will be detected in the CB-TAPS, whereas the deuterons will be mainly detected in the wire chambers surrounding the Crystal Ball, and identified based on the TOF and energy loss in the

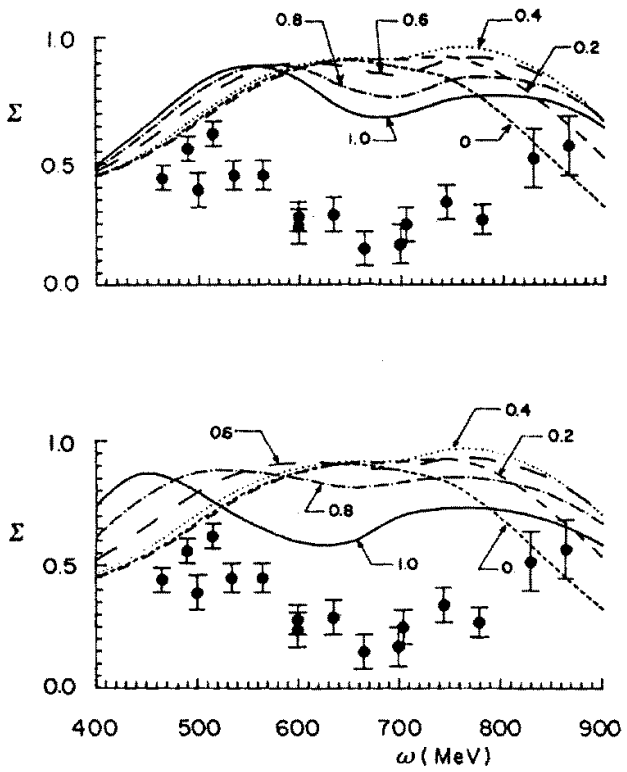

Figure 11: Energy dependence of the beam analyzing power Σ for the reaction $\gamma d \rightarrow \pi^0 d$ at θ^{π}_{CM}=130° [12]. Top: The theoretical curves correspond to different values of the pseudoscalar coupling parameter λ in the πNN vertex [13]. The latter is used to calculate the deuteron wave function. λ=0 corresponds to pure pseudoscalar coupling; λ=1 corresponds to pure psedovector coupling. Bottom: The theoretical curves correspond to different psedoscalar coupling in both the deuteron wave function, and the elementary pion photoproduction operator. The data are from [14–16].

PID detectors. The forward scattered deuterons will be detected in the TAPS detector and identified based on the TOF and energy loss. We will select our good events based on both final-state particles detected. This will allow for stringent kinematic cuts and basically background-free sample. In this way the extraction of the polarization observables will be greatly facilitated because background subtraction will not be needed.

4.2 Target

For the measurement of $\frac{d\sigma}{d\Omega}$ and Σ we will use the current unpolarized LD_2 target. For the measurement of the target analyzing powers we will use a C_4D_9OD frozen-spin target which is very similar to the Bonn frozen-spin target. We will need longitudinally and transversely polarized targets, as well as a target with turnable polarization axis with respect to the beam direction.

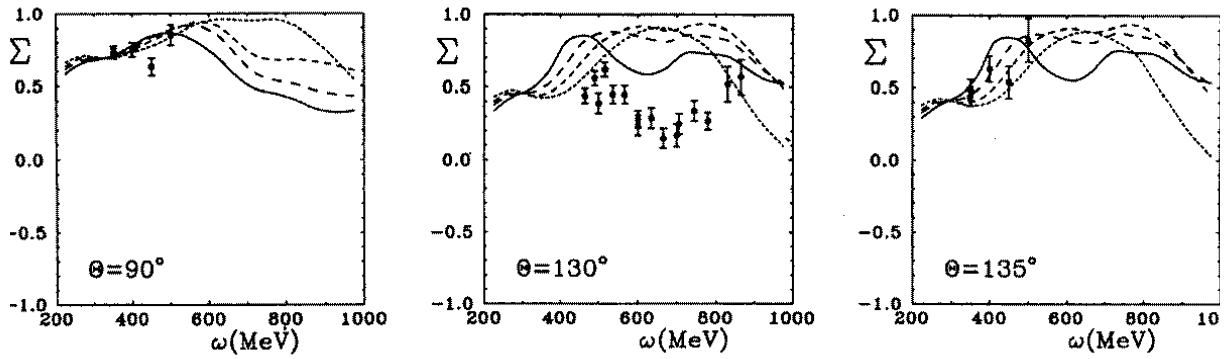

Figure 12: Theoretical predictions from the model of [4] for the energy dependence of Σ at pion CM angle of 90°, 130°, and 135°. Short dashed curve: λ=0 (pure pseudoscalar coupling in the πNN vertex for calculating the deuteron wave function and in the elementary pion photoproduction amplitude), dashed curve: λ=0.6, long-dashed curve: λ=0.8, solid curve: λ=1 (pure pseudovector coupling).

4.3 Trigger

We will mainly trigger on the photons from the pion decay, but triggering on the deuteron can be added as well, depending on the dead time.

4.4 Luminosity

Our beam-time request estimates, based on required statistics, are done assuming 6.5×10^7 γ/s photon flux over the tagged energy range 0.5–1.5 GeV. We assume the frozen-spin deuterium target contains 0.6×10^{23} nuclei/cm^2.

5 Experimental Method

5.1 Measurement of the beam analyzing power Σ

The measurement of Σ is based on (10). At fixed polarization of the photon beam, the φ distribution of the scattered deuterons/pions will be measured for each $(E_\gamma, \cos\theta_{CM})$ bin. The distribution will be fitted by the function $A+B\cos 2\varphi$. Then, $\Sigma(E_\gamma, \cos\theta_{CM})$ will be determined as

$$\Sigma = \frac{1}{P_{lin}}\frac{B}{A}$$

In order to estimate the beam-time request, we used the published data for Σ at 135° and the CLAS unpolarized cross sections. At 0.8 GeV and $\cos\theta^\pi_{CM}$=-0.85, where $\Delta(E_\gamma)$=25 MeV,

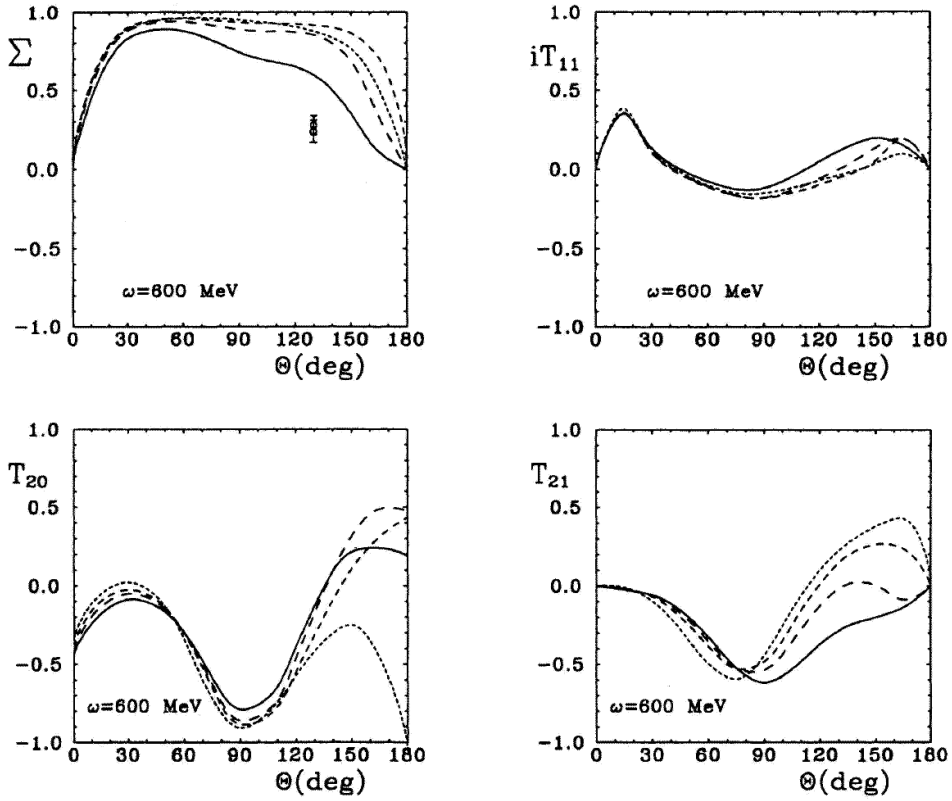

Figure 13: Theoretical predictions from the model of [4] for Σ, iT_{11}, T_20, and T_{22} at E_γ=0.6 GeV.

$\Delta(\cos\theta_{CM})$=0.1, Σ=0.2, and P_{lin}=0.4, we will achieve a statistical uncertainty for Σ of 18% after 600 hours of data taking. For the same running time, at 1. GeV and $\cos\theta^{\pi}_{CM}$=-0.85, where $\Delta(E_\gamma)$=100 MeV, $\Delta(\cos\theta_{CM})$=0.1, Σ=0.5, and P_{lin}=0.1, we will achieve a statistical uncertainty of 47%. The latter case is somewhat extreme, since it combines low cross section with low polarization. The statistical uncertainty of Σ at 1. GeV, but smaller pion CM angles will be better.

5.2 Measurement of the target tensor analyzing power T_{20}

The measurement of T_{20} is based on (8). There, one can see that at β=0° (longitudinally polarized target) all other analyzing powers vanish and T_{20} is enhanced. The determination of T_{20} is very sensitive to misalignments of the beam. In order to eliminate significant contributiona from the other analyzing powers, the target polarization axis must be collinear with the beam direction within 1°. At fixed target polarization and $(E_\gamma, \cos\theta_{CM})$ bin

$$T_{20} = \frac{\sqrt{2}}{p_{zz}}(\frac{\sigma - \sigma_0}{\sigma_0}),$$

where σ_0 and σ are the unpolarized and the polarized cross sections, respectively. This analyzing power does not create azymuthal asymmetries. Thus, its determination is based either on mea-

surements of polarized cross sections at different target polarizations (flipping the polarization regularly, for example), or on measurement of polarized (fixed polarization) and unpolarized cross sections. In case we adopt the latter method, and taking into account, that there are no previous measurements of this variable (we used the predictions of [4] for counting rate estimates, but these might be incorrect, especially at higher energies), we will need 400 hours in total (200 for σ_0, and 200 for σ) to achieve a statistical uncertainty between 16% and 30% at E_γ=0.6 GeV, if T_{20}=-0.8. Smaller values of T_{20} increase the uncertainty linearly. These estimates are based on 45% vector polarization of the target, *i.e.* 16% tensor polarization. We expect the major systematic contribution to come from the target polarization determination.
The measurement of T_{20} is very important, because the extracted values will be used later for determining the other target polarization observables. If the above requested time does not provide statistical uncertainties of less than 30%, more beam time will be requested.

5.3 Measurement of the target vector analyzing power iT_{11} and the tensor analyzing power T_{22}

These analyzing powers will be measured with transversely polarized target: β=90°. At this geometry the parameter T_{21} vanishes and

$$\sigma = \sigma_0[1 + iT_{11}\sqrt{3}p_z cos\varphi - \frac{T_{20}p_{zz}}{2\sqrt{2}} - \frac{\sqrt{3}}{2}T_{22}p_{zz}cos2\varphi]$$

For each $(E_\gamma, \cos\theta_{CM})$ bin, the φ distribution of the deuteron (pion) will be measured, and the analyzing powers will be determined from a fit with the following function $A + Bcos\varphi - Ccos2\varphi$, where

$$A = \sigma_0[1 - \frac{T_{20}p_{zz}}{2\sqrt{2}}]$$
$$B = \sigma_0[iT_{11}\sqrt{3}p_z]$$
$$C = \sigma_0[\frac{\sqrt{3}}{2}T_{22}p_{zz}]$$

By using the previously measured values of T_{20}, the unpolarized cross section can be eliminated from the above relations. We estimate 600 hours of data taking to provide 20% statistical uncertainty of iT_{11} at E_γ=0.8 GeV and $\cos\theta^\pi_{CM}$=-0.85 (ΔE_γ=0.025 GeV), and of 13% at E_γ=1. GeV and $\cos\theta^\pi_{CM}$=-0.85 (ΔE_γ=0.1 GeV). The statistical uncertainties of T_{22} are larger because the tensor polarization is smaller than the vector polarization, so that we will need to use wider photon-energy binning.

5.4 Measurement of the target tensor analyzing power T_{21}

The optimal target geometry for the measurement of T_{21} is when the quantization axis is at β=54.7° with respect to the beam axis. In this case T_{20} vanishes. The method is similar to the one used for determining iT_{11} and T_{22}. In this case, the polarized cross section for given $(E_\gamma, \cos\theta_{CM})$ bin is expressed as

$$\sigma = \sigma_0[1 + iT_{11}\sqrt{3}p_z \sin 54.7 cos\varphi + \sqrt{3}T_{21}p_{zz}\sin 54.7\cos 54.7\sin\varphi - \frac{\sqrt{3}}{2}T_{22}p_{zz}\sin^2 54.7 cos2\varphi]$$

T_{21} will be defined after fitting a function $A + Bcos\varphi + C\sin\varphi - Dcos2\varphi$ to the azymuthal distribution of the final state deuteron/pion for each $(E_\gamma, \cos\theta_{CM})$ bin, and determining the fit parameters. We estimate that 600 hours of data taking will provide statistical uncertainties of up to 50% with wide energy binning. This time can be reduced if the frozen-spin target can be produced with larger density.

6 Beam time request

- 75 h with unpolarized beam and target for measurement of $\frac{d\sigma}{d\Omega}$. We can run simultaneously with the proposed experiment of Briscoe *et al.*.
- 600 h with linearly polarized beam for measurement of Σ. We can run simultaneously with the proposed experiment of Briscoe *et al.*.
- 400 h with longitudinally polarized target and unpolarized beam for measurement of T_{20} We can run simultaneously with the proposed experiment of Pedroni *et al.* with circularly polarized beam.
- 600 h with transversely polarized target and unpolarized beam for measurement of iT_{11} and T_{22}.
- 600 h with polarized target with quantization axis at 54.7° with respect to the beam axis for measurement of T_{21}.

References

[1] Y. Ilieva for the CLAS Collaboration, Nucl. Phys. **A737**, S158 (2004)

[2] A. Imanishi *et al.*, Phys. Rev. Lett. **54**, 2497 (1985)

[3] T. Miyachi, H. Tezuka, and Y. Morita, Phys. Rev. C **36**, 844 (1987)

[4] H. Garcilazo and E. Moya de Guerra, Phys. Rev. C **52**, 49 (1995)

[5] A.E. Kudryavtsev *et al.*, Phys. Rev. C **71**, 035202 (2005)

[6] A. Fix, *private communication* (2005)

[7] A. Fix and H. Arenhövel, Nucl. Phys. **A697**, 277 (2002)

[8] G.A. Sokol *et al.*, arXiv:nucl-ex/0106005

[9] S.J. Brodsky *et al.*, Phys. Rev. C **64**, 055204 (2001)

[10] D.G. Meekins *et al.*, Phys. Rev. C **60**, 052201 (1999)

[11] E. Leader, *Spin in particle physics*, Cambride University Press (2001)

[12] H. Garcilazo and E. Moya de Guerra, Phys. Rev. C **49**, R601 (1994)

[13] W. W. Buck, F. Gross, Phys. Rev. D **20**, 2361 (1979)

[14] K. Ukai and T. Nakamura, Institute for Nuclear Study, University of Tokyo, Japan, Report No. INS-TEC-22 (1985)

[15] G. V. Holtey *et al.*, Z. Phys. **259**, 51 (1973)

[16] F. V. Adamyan *et al.*, JETP Lett. **39**. 711 (1984)